

# Modulation of Electronic Coupling through Self-Assembled Monolayers via Internal Chemical Modification

Jun Cheng, Gotthard Sàghi-Szabó, John A. Tossell, and Cary J. Miller\*

Contribution from the Department of Chemistry and Biochemistry, University of Maryland, College Park, Maryland 20742

Received September 20, 1995®

**Abstract:** Self-assembled monolayers of  $\omega$ -hydroxyalkanethiols at Au electrodes are used to probe the structural dependence of long-range electron transfer. The electron transfer rates for ferricyanide and osmium(III) tris(bipyridyl) are measured at Au electrodes coated with self-assembled monolayers of  $\text{HO}(\text{CH}_2)_n\text{--X--}(\text{CH}_2)_m\text{SH}$  where X denotes an ether, olefin, or alkyne function. Each of these modifications decreases the electronic coupling across the monolayers. *Ab initio* calculations of the neutral diradical splitting energies for modified and unmodified alkanes correctly predict these decreases in electronic coupling.

## Introduction

The role of the intervening medium between an electron donor and acceptor in controlling the probability of long-range electron transfer is a question of considerable importance to a number of diverse scientific and technological research areas. These areas range from understanding long-range electron transfers in biochemical systems to designing molecular based electronic devices.<sup>1</sup> A serious deficiency in the current understanding of long-range electron transfer is how each atom and each bond within the intervening medium affects the long-range electronic coupling. Advances in this field have been slow due in part to the difficulty of making experimental measurements of long-range electron transfer rates in rigid, well-defined structures. Much of the experimental work in this area has been done using donor/acceptor pairs connected by rigid spacer groups.<sup>2</sup> The required rigidity of these spacers is generally achieved by including fused ring systems, hydrogen bonding, and other interactions which necessarily increase the chemical and structural complexity of the spacer. Apart from the increased synthetic challenges in making systematic structural modifications, the increased chemical complexity seriously impedes the detailed theoretical description of the electronic coupling in these systems.

An alternate strategy in probing these long-range electron transfer reactions is to utilize self-assembled thiol monolayers adsorbed on Au surfaces.<sup>3</sup> The structure of these thiol monolayers has been the subject of considerable study in recent years.<sup>4</sup> For simple alkanethiol monolayers, the crystalline *all-trans*

structure is enforced by the packing of the alkyl chains.<sup>5</sup> The electronic coupling within these monolayers (particularly the hydrocarbon chain length dependence of the electronic coupling) has been determined using electron transfer rate measurements from the underlying Au electrode to tethered redox sites at the monolayer/electrolyte solution interface.<sup>6</sup> These results have been in very good agreement with similar measurements of homogeneous electron transfer rates between donor/acceptor pairs separated by rigid hydrocarbon spacers.<sup>7</sup>

We have employed  $\omega$ -hydroxyalkanethiol monolayers at gold electrodes as electron tunneling barriers to characterize solution redox species.<sup>8</sup> Analysis of the electron transfer data at these monolayer insulated electrodes provides reorganization energies and electronic coupling parameters which reveal how the structure of a redox molecule governs its electron transfer reactivity.<sup>9</sup> In this paper we describe another important application of these monolayer coated electrodes as a direct probe of the structural dependence of long-range electronic coupling. By introducing subtle chemical modifications within the alkyl segment of the  $\omega$ -hydroxyalkanethiol monolayer, we probe *at the atom level* how such modifications affect the long-range electron transfer. The single ether, olefin, and alkyne modifica-

(3) (a) Nuzzo, R. G.; Allara, D. L. *J. Am. Chem. Soc.* **1983**, *105*, 4481–4483. (b) Sabatani, E.; Rubinstein, I.; Maoz, R.; Sagiv, J. *J. Electroanal. Chem.* **1987**, *219*, 365–371. (c) Porter, M. D.; Bright, T. B.; Allara, D. L.; Chidsey, C. E. D. *J. Am. Chem. Soc.* **1987**, *109*, 3559–3568. (d) Bain, C. D.; Troughton, E. B.; Tao, Y. T.; Evall, J.; Whitesides, G. M.; Nuzzo, R. G. *J. Am. Chem. Soc.* **1989**, *111*, 321–335.

(4) (a) Strong, L.; Whitesides, G. M. *Langmuir* **1988**, *4*, 546–558. (b) Chidsey, C. E. D.; Liu, G.-Y.; Rowntree, P.; Scoles, G. *J. Chem. Phys.* **1989**, *91*, 4421–4423. (c) Fenter, P.; Eberhardt, A.; Eisenberger, P. *Science* **1994**, *266*, 1216–1218.

(5) (a) Nuzzo, R. G.; Fusco, F. A.; Allara, D. L. *J. Am. Chem. Soc.* **1987**, *109*, 2358–2368. (b) Ulman, A.; Eilers, J. E.; Tillman, N. *Langmuir* **1989**, *5*, 1147–1152.

(6) (a) Li, T. T.-T.; Weaver, M. J. *J. Am. Chem. Soc.* **1984**, *106*, 6107–6108. (b) Chidsey, C. E. D. *Science* **1991**, *251*, 919–922. (c) Rowe, G. K.; Creager, S. E. *Langmuir* **1991**, *7*, 2307–2312. (d) Finklea, H. O.; Hanshew, D. D. *J. Am. Chem. Soc.* **1992**, *114*, 3173–3181.

(7) (a) Closs, G. L.; Calcaterra, L. T.; Green, N. J.; Penfield, K. W.; Miller, J. R. *J. Phys. Chem.* **1986**, *90*, 3673–3683. (b) Beratan, D. N. *J. Am. Chem. Soc.* **1986**, *108*, 4321–4326. (c) Oevering, H.; Paddon-Row, M. N.; Heppener, M.; Oliver, A. M.; Cotsaris, E.; Verhoeven, J. W.; Hush, N. S. *J. Am. Chem. Soc.* **1987**, *109*, 3258–3269. (d) Paddon-Row, M. N.; Oliver, A. M.; Warman, M.; Smit, K. J.; de Haas, M. P.; Oevering, H.; Verhoeven, J. W. *J. Phys. Chem.* **1988**, *92*, 6958–6962.

(8) (a) Miller, C.; Cuendet, P.; Grätzel, M. *J. Phys. Chem.* **1991**, *95*, 877–886. (b) Miller, C.; Grätzel, M. *J. Phys. Chem.* **1991**, *95*, 5225–5233.

(9) Terrettaz, S.; Becka, A. M.; Traub, M. J.; Fettingner, J. C.; Miller, C. *J. J. Phys. Chem.* **1995**, *99*, 11216–11224.

® Abstract published in *Advance ACS Abstracts*, January 1, 1996.

(1) (a) *Structure and Bonding: Long Range Electron Transfer in Biology*, Springer-Verlag: New York, 1991; Vol. 75. (b) *Metal Ions in Biological Systems: Electron Transfer Reactions in Metalloproteins*, Sigel, H., Sigel, A., Eds.; Marcel Dekker: New York, 1991; Vol. 27. (c) Newton, M. D. *Chem. Rev.* **1991**, *91*, 767–792. (d) Winkler, J. R.; Gray, H. B. *Chem. Rev.* **1992**, *92*, 369–379. (e) *Molecular Electronics-Science and Technology: AIP Conference Proceedings*; Aviram, A., Ed.; American Institute of Physics: New York, 1992; Vol. 262.

(2) (a) Hush, N. S.; Paddon-Row, M. N.; Cotsaris, E.; Overing, H.; Verhoeven, J. W.; Heppener, M. *Chem. Phys. Lett.* **1985**, *117*, 8–11. (b) Liang, N.; Miller, J. R.; Closs, G. L. *J. Am. Chem. Soc.* **1990**, *112*, 5353–5354. (c) Vassilian, A.; Wishart, J. F.; Hemelryck, B. V.; Schwarz, H.; Isied, S. S. *J. Am. Chem. Soc.* **1990**, *112*, 7278–7296. (d) Paulson, B.; Pramod, K.; Eaton, P.; Closs, G. L.; Miller, J. R. *J. Phys. Chem.* **1993**, *97*, 13042–13045. (e) Ogawa, M. Y.; Wishart, J. F.; Young, Z.; Miller, J. R.; Isied, S. S. *J. Phys. Chem.* **1993**, *97*, 11456–11463. (f) Larson, S. L.; Hendrickson, S. M.; Ferrere, S.; Derr, D. L.; Elliott, C. M. *J. Am. Chem. Soc.* **1995**, *117*, 5881–5882. (g) Meade, T. J.; Kayyem, J. F. *Angew. Chem., Int. Ed. Engl.* **1995**, *34*, 352–354.

tions studied here represent some of the simplest structural modifications possible. Even so, their affect on the electronic coupling through the hydrocarbon chain is not easily predicted. Indeed, a large motivation for these measurements is to serve as reference points for *ab initio* calculations of long-range electronic coupling.<sup>10</sup> Following previous *ab initio* approaches, we calculate diradical splitting energies from which relative tunneling rates are determined.<sup>11</sup> These *ab initio* predictions are compared with the measured electron tunneling rates.

## Experimental Section

**Syntheses.** (a) **14-Hydroxytetradecane-1-thiol** ( $C_{14}$ ) was synthesized from 1,14-tetradecanediol as previously described.<sup>12</sup> <sup>1</sup>H NMR (200 MHz,  $CDCl_3$ )  $\delta$  3.56 (t, 2H,  $-CH_2-OH$ ), 2.46 (q, 2H,  $-CH_2-SH$ ); <sup>13</sup>C NMR (200 MHz,  $CDCl_3$ )  $\delta$  62.7 ( $-CH_2-OH$ ), 33.9 ( $-CH_2-SH$ ); IR (KBr pellets) 3294 (broad O-H stretch), 2919, 2844  $cm^{-1}$  (C-H stretches).

(b) **14-Hydroxy-*x*-oxotetradecane-1-thiol** ( $E_{14}^x$ ,  $x = 6, 7, 8$ ). All of  $E_{14}^x$  were synthesized from the corresponding alkanediols and dibromides as previously described.<sup>13</sup> Spectral characterization of  $E_{14}^7$ : <sup>1</sup>H NMR (200 MHz,  $CDCl_3$ )  $\delta$  3.39 (t, 4H,  $-CH_2-O-CH_2-$ ), 3.58 (t, 2H,  $-CH_2-OH$ ), 2.48 (q, 2H,  $-CH_2-SH$ ); <sup>13</sup>C NMR (200 MHz,  $CDCl_3$ )  $\delta$  70.8, 71.0 ( $-CH_2-O-CH_2-$ ), 62.8 ( $-CH_2-OH$ ), 34.2 ( $-CH_2-SH$ ); IR (KBr pellets) 1119 (C-O-C, C-O stretch), 3425 (broad O-H stretch), 2938, 2856  $cm^{-1}$  (C-H stretches).

(c) **14-Hydroxy-7-tetradecyne-1-thiol** ( $T_{14}^7$ ). The synthesis of  $T_{14}^7$  was achieved by the following sequence. 1,6-Hexanediol was converted to 6-iodo-1-hexanol via refluxing the diol in a mixture of octane and 51% aqueous HI. After purification, the alcohol was protected via reaction with dihydropyran<sup>14</sup> and reacted with acetylene according to the method of Beckmann *et al.*<sup>15</sup> to form 1-tetrahydropyranyloxy-7-octyne. This terminal alkyne was alkylated with 6-chloro-1-iodohexane as described by Schwarz *et al.*<sup>16</sup> and Gensler *et al.*<sup>17</sup> to give 1-tetrahydropyranyloxy-14-chloro-7-tetradecyne. After deprotection of the alcohol,<sup>14</sup> the chloride was converted to the thiol using alcoholic thiourea followed by treatment in base as described previously.<sup>12</sup> <sup>1</sup>H NMR (200 MHz,  $CDCl_3$ )  $\delta$  2.12 (m, 4H,  $-CH_2-CC\equiv CH_2-$ ), 3.61 (t, 2H,  $-CH_2-OH$ ), 2.50 (q, 2H,  $-CH_2-SH$ ); <sup>13</sup>C NMR (200 MHz,  $CDCl_3$ )  $\delta$  80.1, 80.3 ( $-C\equiv C-$ ), 62.9 ( $-CH_2-OH$ ), 33.9 ( $-CH_2-SH$ ); IR (KBr pellets) 3425 (broad O-H stretch), 2931, 2856  $cm^{-1}$  (C-H stretches).

(d) **14-Hydroxy-(*E*)-7-tetradecene-1-thiol** ( $D_{14}^7$ ) was synthesized from 14-hydroxy-7-tetradecyne-1-thiol via Na reduction in liquid  $NH_3$  using the method of Schwarz *et al.*<sup>16</sup> <sup>1</sup>H NMR (200 MHz,  $CDCl_3$ )  $\delta$  5.40 (m, 2H,  $-CH=CH-$ ), 1.96 (m, 4H,  $-CH_2-CH=CH-CH_2-$ ), 3.60 (t, 2H,  $-CH_2-OH$ ), 2.48 (q, 2H,  $-CH_2-SH$ ); <sup>13</sup>C NMR (200 MHz,  $CDCl_3$ )  $\delta$  130.2, 130.5 ( $-CH=CH-$ ), 63.0 ( $-CH_2-OH$ ), 34.0 ( $-CH_2-SH$ ); IR (KBr pellets) 969 (*trans*- $CH=CH$ , C-H stretch), 3423 (broad O-H stretch), 2924, 2854  $cm^{-1}$  (C-H stretches).

(e) **Tris(2,2'-bipyridyl)osmium(II) hydrogen sulfate** ( $Os(bpy)_3^{2+}$ ) was synthesized by the reductive ligand substitution of  $K_2OsCl_6$  (Strem

Chemicals) with 2,2'-bipyridine as described by Creutz.<sup>18</sup> The perchlorate salt initially formed was dissolved in  $CH_3CN$  and reprecipitated as the hydrogen sulfate salt via the addition of tetrabutylammonium hydrogen sulfate. All other chemicals were purchased from Aldrich and used as received.

**Electrode Fabrication.** Au electrodes were fabricated by radio frequency sputtering *ca.* 3000 Å from a 99.99% Au target onto microscope slides through a special mask. A *ca.* 500 Å chromium layer was sputtered first to promote adhesion of the gold films. The Au electrodes were cleaned through successive exposures to chromic acid and aqueous HF, rinsed with water, and immediately placed into ethanolic thiol solutions as described previously.<sup>12</sup> The Au electrodes were kept overnight in the *ca.* 30 mM solution of the corresponding  $\omega$ -hydroxyalkanethiols prior to their use in the electrochemical studies. The geometric area of the electrodes was 0.13  $cm^2$ .

**Electrochemical Measurements.** All electrochemical measurements were made using a BAS-100A electrochemical analyzer in solutions which had been purged with  $N_2$  and were held at 0 °C in a jacketed electrochemical cell. The  $Os(bpy)_3^{2+}$  was oxidized *in situ* using ammonium cerium(IV) nitrate prior to its voltammetric characterization. All kinetic measurements were made in aqueous solutions containing 0.25 M  $CF_3COONa$  and 3 mM of the redox molecule. All potentials were measured and are reported versus a saturated calomel electrode.

**Ab Initio Calculations.** *Ab initio* computations were performed using GAMESS.<sup>19</sup> Relying on previous theoretical approaches,<sup>11</sup> we have calculated  $\alpha,\omega$ -diradical splitting energies for the neutral triplet diradical using an unrestricted Hartree-Fock SCF calculation. The geometries of all the *trans*-alkane and modified alkanes were optimized at the 3-21G basis set level prior to the introduction of the radical reporter groups.<sup>20</sup>

## Results and Discussion

Heterogeneous electron transfer rate measurements made at thiol monolayer modified electrodes give a surprisingly easy and accurate way of probing structural influences on long-range electronic coupling. Figure 1 shows a schematic representation of the thiol monolayers investigated. The single internal chemical modifications were centrally located within the hydrocarbon chain of the  $HO(CH_2)_{14}SH$  parent in order to minimize their interactions with either the Au surface or the electrolyte solution. The oxygen, *trans*-olefin, and alkyne groups were chosen because of their compatibility with the *all-trans*  $\omega$ -hydroxyalkanethiol monolayer structure.

The self-assembly of these modified  $\omega$ -hydroxyalkanethiols onto Au electrodes was monitored via surface wetting and capacitance measurements. We find that each of the modified monolayers is completely wetted by water, precluding extensive disruption of the monolayer packing which would expose the hydrophobic alkyl chains.<sup>21</sup> The capacitances of the  $\omega$ -hydroxyalkanethiol monolayer coated electrodes listed in Table 1 are also consistent with a close-packed thiol monolayer. As expected due to the increased polarity or polarizability of the modifying groups, we find higher capacitances for each of the ether, alkene, and alkyne modified monolayers. Additional structural characterization for the ether modified monolayer

(18) Creutz, C.; Chou, M.; Netzel, T. L.; Okumura, M.; Sutin, N. *J. Am. Chem. Soc.* **1980**, *102*, 1309-1319.

(19) Schmidt, M. W.; Baldrige, K. K.; Boatz, J. A.; Elbert, S. T.; Gordon, M. S.; Jensen, J. H.; Koseki, S.; Matsunaga, N.; Nguyen, K. A.; Su, S. J.; Windus, T. L.; Dupuis, M.; Montgomery, J. A. *J. Comput. Chem.*, **1993**, *14*, 1347-1363.

(20) (a) Binkley, J. S.; Pople, J. A.; Hehre, W. J. *J. Am. Chem. Soc.* **1980**, *102*, 939-947. (b) Gordon, M. S.; Binkley, J. S.; Pople, J. A.; Pietro, W. J.; Hehre, W. J. *J. Am. Chem. Soc.* **1982**, *104*, 2797-2803. (c) Pietro, W. J.; Francl, M. M.; Hehre, W. J.; Defrees, D. J.; Pople, J. A.; Binkley, J. S. *J. Am. Chem. Soc.* **1982**, *104*, 5039-5048.

(21) The complete wetting of these modified  $\omega$ -hydroxyalkanethiol monolayer coated electrodes was inferred from the observation of interference fringes as the surface of the electrode was dried in a stream of air.

(10) (a) Paddon-Row, M. N.; Wong, S. S.; Jordan, K. D. *J. Am. Chem. Soc.* **1990**, *112*, 1710-1722. (b) Evenson, J. W.; Karplus, M. *Science* **1993**, *262*, 1247-1249.

(11) (a) Naleway, C. A.; Curtiss, L. A.; Miller, J. R. *J. Phys. Chem.* **1991**, *95*, 8434-8437. (b) Liang, C.; Newton, M. D. *J. Phys. Chem.* **1992**, *96*, 2855-2866. (c) Jordan, K. D.; Paddon-Row, M. N. *J. Phys. Chem.* **1992**, *96*, 1188-1196. (d) Liang, C.; Newton, M. D. *J. Phys. Chem.* **1993**, *97*, 3199-3211. (e) Curtiss, L. A.; Naleway, C. A.; Miller, J. R. *J. Phys. Chem.* **1993**, *97*, 4050-4058.

(12) (a) Becka, A. M.; Miller, C. J. *J. Phys. Chem.* **1992**, *96*, 2657-2668. (b) Becka, A. M.; Miller, C. J. *J. Phys. Chem.* **1993**, *97*, 6233-6239.

(13) Sinniah, K.; Cheng, J.; Terrettaz, S.; Reutt-Robey, J. E.; Miller, C. J. *J. Phys. Chem.* **1995**, *99*, 14500-14505.

(14) Miyashita, M.; Yoshikoshi, A.; Grieco, P. J. *Org. Chem.* **1977**, *42*, 3772-3774.

(15) Beckmann, W.; Doerjer, G.; Logemann, E.; Merkel, C.; Schill, G.; Zürcher, C. *Synthesis*, **1975**, 423-425.

(16) Schwarz, M.; Waters, R. M. *Synthesis* **1972**, 567-568.

(17) Gensler, W. J.; Prasad, R. S.; Chaudhuri, A. P.; Alam, I. *J. Org. Chem.* **1979**, *44*, 3643-3652.

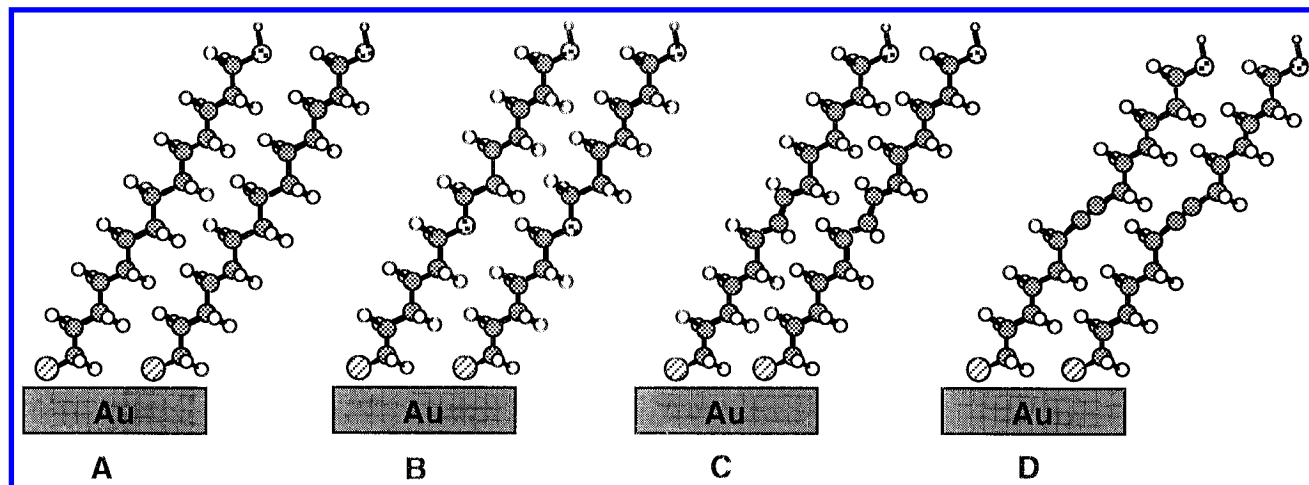


**Figure 1.** Schematic representation of the self-assembled  $\omega$ -hydroxyalkanethiol monolayers adsorbed on the Au surface: HS(CH<sub>2</sub>)<sub>14</sub>OH, (A); HS(CH<sub>2</sub>)<sub>6</sub>O(CH<sub>2</sub>)<sub>7</sub>OH (B); *trans*-HS(CH<sub>2</sub>)<sub>6</sub>CH=CH(CH<sub>2</sub>)<sub>6</sub>OH, (C); HS(CH<sub>2</sub>)<sub>6</sub>C≡C(CH<sub>2</sub>)<sub>6</sub>OH (D).

**Table 1.** Capacitances and Relative Electron Tunneling Rates for the  $\omega$ -Hydroxyalkanethiol Monolayers<sup>a</sup>

molecular structure	capacitance ( $\mu\text{F}/\text{cm}^2$ ) ( $m^b$ )	$k_m/k_{um}$	
		Fe(CN) <sub>6</sub> <sup>3-</sup> ( $m^b$ )	Os(bpy) <sub>3</sub> <sup>3+</sup> ( $m^b$ )
HO(CH <sub>2</sub> ) <sub>14</sub> SH	1.60 ± 0.07 (27)	1	1
HO(CH <sub>2</sub> ) <sub>7</sub> O(CH <sub>2</sub> ) <sub>6</sub> SH	1.84 ± 0.07 (15)	0.68 ± 0.08 (12)	0.66 ± 0.14 (6)
HO(CH <sub>2</sub> ) <sub>6</sub> O(CH <sub>2</sub> ) <sub>7</sub> SH	1.91 ± 0.12 (10)	0.70 ± 0.11 (12)	0.57 ± 0.09 (6)
HO(CH <sub>2</sub> ) <sub>8</sub> O(CH <sub>2</sub> ) <sub>5</sub> SH	1.85 ± 0.06 (7)	0.77 ± 0.16 (14)	0.50 ± 0.06 (4)
HO(CH <sub>2</sub> ) <sub>6</sub> CH=CH(CH <sub>2</sub> ) <sub>6</sub> SH	1.78 ± 0.09 (15)	0.28 ± 0.08 (21)	0.41 ± 0.07 (10)
HO(CH <sub>2</sub> ) <sub>6</sub> C≡C(CH <sub>2</sub> ) <sub>6</sub> SH	1.92 ± 0.16 (14)	0.38 ± 0.05 (22)	0.77 ± 0.15 (8)

<sup>a</sup> The average ratios of the heterogeneous electron transfer rates for the Fe(CN)<sub>6</sub><sup>3-</sup> and Os(bpy)<sub>3</sub><sup>3+</sup> couples measured at the modified monolayers relative to that measured at the unmodified HO(CH<sub>2</sub>)<sub>14</sub>SH monolayer are listed along with the standard deviations. <sup>b</sup>  $m$  denotes the number of independent measurements used to determine the value.

films was supplied by infrared reflection–adsorption measurements which indicate that the introduction of the ether function results in no measurable change in the monolayer tilt angle and a slight, 10°, reduction in the monolayer twist angle.<sup>13</sup> Initial attempts at characterizing the structure of the alkyne modified monolayers via infrared measurements have been hampered by significant broadening of the CH<sub>2</sub> bands caused by the alkyne group. This broadening along with a significant decrease in the CH<sub>2</sub> band intensities has impeded the accurate integration of the infrared bands required for the orientational analysis. Broadening of the CH<sub>2</sub> bands was also observed for the ether modification. In that case the broadening was ascribed to the presence of the ether group within  $\omega$ -hydroxyalkanethiol rather than disorder caused by the modifying group.

Heterogeneous electron transfer rate measurements of solution redox probes made at these  $\omega$ -hydroxyalkanethiol monolayers are also consistent with the formation of low defect density monolayers. The electron transfer rates for Fe(CN)<sub>6</sub><sup>3-</sup> and Os(bpy)<sub>3</sub><sup>3+</sup> were obtained from the linear sweep voltammograms after correction for both diffusion limitations and the double layer effect as described previously,<sup>9, 12</sup> (Figures 2 and 3). In every instance, the internally modified monolayers give smaller electron transfer rates, indicating that these modified  $\omega$ -hydroxyalkanethiol monolayers block the long-range electron transfer more efficiently than the parent  $\omega$ -hydroxyalkanethiol monolayer.<sup>22</sup>

The differences in the electron transfer rates measured at these monolayer coated electrodes are due primarily to a change in

(22) If these modifications resulted in more highly defective monolayers, one might expect an increase in the electron transfer rate for a solution species. Because a HO(CH<sub>2</sub>)<sub>14</sub>SH monolayer decreases the heterogeneous electron transfer rate of solution species by over six orders of magnitude, even a small number of defects allowing a closer approach of the redox molecule to the electrode surface could result in significantly larger currents.

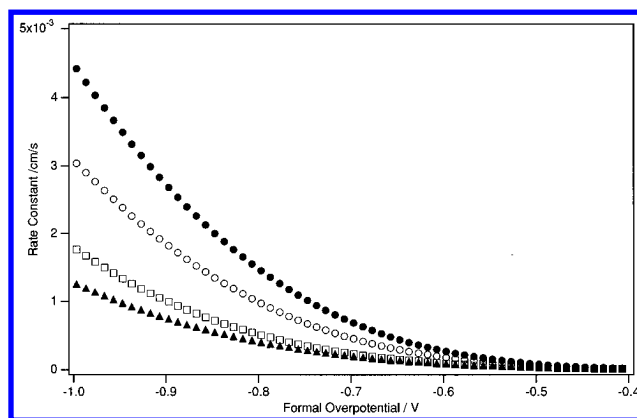


**Figure 2.** Heterogeneous electron transfer rates versus the formal overpotential for Fe(CN)<sub>6</sub><sup>3-</sup> measured at Au electrodes coated with  $\omega$ -hydroxyalkanethiol monolayers: HS(CH<sub>2</sub>)<sub>14</sub>OH (●); HS(CH<sub>2</sub>)<sub>6</sub>O(CH<sub>2</sub>)<sub>7</sub>OH (○); HS(CH<sub>2</sub>)<sub>6</sub>C≡C(CH<sub>2</sub>)<sub>6</sub>OH (□); *trans*-HS(CH<sub>2</sub>)<sub>6</sub>CH=CH(CH<sub>2</sub>)<sub>6</sub>OH (▲). These data were obtained from cyclic voltammograms measured at 5.12 V/s in aqueous solutions of 0.25 M CF<sub>3</sub>COONa at 0 °C.

the electronic coupling across the monolayers.<sup>23</sup> By comparing the heterogeneous electron transfer rate constants, one can gauge how these subtle chemical modifications affect the long-range electronic coupling through the organized monolayers (Table

(23) The heterogeneous electron transfer rate measured at these thiol modified electrodes depends on both the electronic coupling between the electrode and redox probe and the reorganization energy of the redox probe. A potential problem with comparing heterogeneous electron transfer rates between different monolayer coated electrodes is that the reorganization energy of a redox probe may vary at each of the electrodes due to varying degrees of electrostatic screening of the redox probe by the electrode image charge. For the monolayers studied in this work, these image charge effects are anticipated to be negligible. (See Liu, Y.-P.; Newton, M. D. *J. Phys. Chem.* **1994**, 98, 7162–7169.)

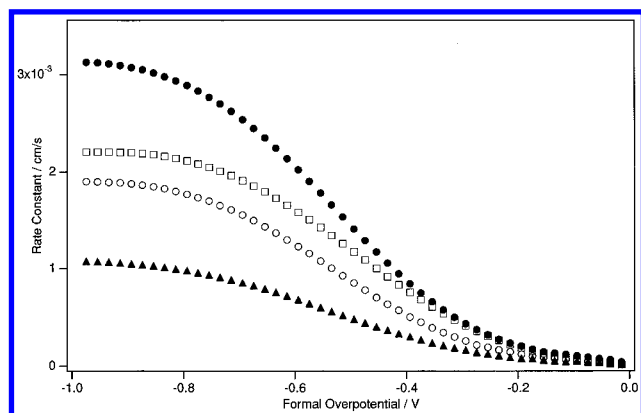


**Figure 3.** Heterogeneous electron transfer rates versus the formal overpotential for  $\text{Os}(\text{bpy})_3^{3+}$  measured at Au electrodes coated with  $\omega$ -hydroxyalkanethiol monolayers:  $\text{HS}(\text{CH}_2)_{14}\text{OH}$  (●);  $\text{HS}(\text{CH}_2)_6\text{O}(\text{CH}_2)_7\text{OH}$  (○);  $\text{HS}(\text{CH}_2)_6\text{C}\equiv\text{C}(\text{CH}_2)_6\text{OH}$  (□); *trans*- $\text{HS}(\text{CH}_2)_6\text{CH}=\text{CH}(\text{CH}_2)_6\text{OH}$  (▲). These data were obtained from cyclic voltammograms measured at 5.12 V/s in aqueous solutions of 0.25 M  $\text{CF}_3\text{COONa}$  at 0 °C.

1). The relative heterogeneous electron transfer rates are not a strong function of the applied potential so that a single average relative rate is given for each modification. The electronic coupling is highest for the unmodified  $\omega$ -hydroxyalkanethiol. The electronic coupling of the ether modified monolayer is smaller and independent of whether the oxygen is positioned at the 6, 7, or 8 position along the alkyl chain.<sup>24</sup> The electronic coupling decreases by approximately a factor of 3 when a single *trans*-olefin is introduced. This is a slightly greater decrease than would be caused by increasing the monolayer length by one methylene unit.<sup>12</sup> The single alkyne modification reduces the electronic coupling less than that observed for the olefin. Except for the alkyne modified monolayer, the relative ratios determined using  $\text{Fe}(\text{CN})_6^{3-}$  and  $\text{Os}(\text{bpy})_3^{3+}$  are in reasonable agreement. The discrepancy in the electronic coupling ratio for the alkyne using the two redox couples is most likely due to some penetration of the more hydrophobic Os complex within the alkyne monolayer. In order to probe for the penetration of the redox complexes at monolayer defect sites, we have repeated these voltammetric experiments in the presence of 1.5 mM 1-octanol. This amphiphile was previously found to act as a competitive binder for these defect sites.<sup>12a</sup> Except for the reduction rate for  $\text{Os}(\text{bpy})_3^{3+}$  measured at the alkyne modified monolayer, we observe little change in these electron transfer rates measured in the presence of 1-octanol. The alkyne modified monolayer coated electrode rates decrease by approximately 40%, lowering the relative electronic coupling to a value close to that measured using ferricyanide.

The decreases in the electronic coupling caused by these internal modifications may seem surprising especially for the olefin and alkyne modifications. One may have expected the  $\pi$  and  $\pi^*$  orbitals to couple the electron through the thiol monolayer more efficiently due to their smaller HOMO/LUMO energy gap when compared with the  $\sigma$  and  $\sigma^*$  orbitals available in the unmodified monolayer. However, because these modifications are buried within the monolayer, the electronic coupling of the electrode and redox orbitals by the orbitals of the modification would involve two long through-space interactions.

(24) Whether the ether function is positioned at an even or odd site along the hydrocarbon chain does affect the measured electron transfer rates for charged redox probes via a change in the electrode's potential of zero charge (pzc). We observe a *ca.*  $\pm 130$  mV shift in the pzc for the ether modified thiol monolayers relative to the unmodified  $\omega$ -hydroxyalkanethiol. (Please see ref 13.) The systematic differences in the measured electron transfer rates caused by this electrostatic effect are largely eliminated by the double layer correction.

**Table 2.** Comparison between *ab Initio* Electronic Coupling Calculations and Experiments<sup>a</sup>

molecular structure	$\Delta E_{\text{an}}$ (mH)	$\Delta E_{\text{cat}}$ (mH)	$k_{\text{th}}^b$	$k_{\text{ex}}^b$
$\bullet\text{CH}_2(\text{CH}_2)_3\text{CH}_2(\text{CH}_2)_3\text{CH}_2\bullet$	4.158	10.330	1	1
$\bullet\text{CH}_2(\text{CH}_2)_3\text{O}(\text{CH}_2)_3\text{CH}_2\bullet$	3.389	6.214	0.44	0.67
$\bullet\text{CH}_2(\text{CH}_2)_3\text{CH}=\text{CH}(\text{CH}_2)_3\text{CH}_2\bullet$	-2.691	-7.718	1	1
$\bullet\text{CH}_2(\text{CH}_2)_3\text{CH}=\text{CH}(\text{CH}_2)_3\text{CH}_2\bullet$	-1.174	-4.186	0.27	0.35
$\bullet\text{CH}_2(\text{CH}_2)_3\text{C}\equiv\text{C}(\text{CH}_2)_3\text{CH}_2\bullet$	8.730	15.696	5.5	0.38 <sup>c</sup>
$\text{Li CH}_3(\text{CH}_2)_3\text{CH}_2(\text{CH}_2)_3\text{CH}_3 \text{ Li}$	0.01340	0.01185	1	1
$\text{Li CH}_3(\text{CH}_2)_3\text{O}(\text{CH}_2)_3\text{CH}_3 \text{ Li}$	0.01096	0.00870	0.61	0.67
$\text{Li CH}_3(\text{CH}_2)_3\text{CH}_2\text{CH}_2(\text{CH}_2)_3\text{CH}_3 \text{ Li}$	-0.00771	-0.00703	1	1
$\text{Li CH}_3(\text{CH}_2)_3\text{CH}=\text{CH}(\text{CH}_2)_3\text{CH}_3 \text{ Li}$	-0.00567	-0.00472	0.50	0.35
$\text{Li CH}_3(\text{CH}_2)_3\text{C}\equiv\text{C}(\text{CH}_2)_3\text{CH}_3 \text{ Li}$	0.00547	0.00468	0.47	0.38 <sup>c</sup>

<sup>a</sup> The theoretical relative rates were calculated from the sum of the anion and cation splitting energies. (See text.) The experimental relative rates were taken as the average relative rates from Table 1.

<sup>b</sup>  $k_{\text{th}}$  and  $k_{\text{ex}}$  denote the theoretical and experimental relative rates, respectively. <sup>c</sup> This relative ratio was taken as being equal to that obtained from the  $\text{Fe}(\text{CN})_6^{3-}$  data in Table 1.

This direct interaction is not an effective electronic coupling pathway for the electron through the monolayer. Indeed, several groups have presented theoretical analyses of the electronic coupling through saturated hydrocarbon spacers and concluded that the electronic coupling in these systems should be dominated by the overlap and energy matching between orbitals located on nearby atoms.<sup>11</sup> The direct electronic coupling beyond these 1st-, 2nd-, and 3rd-nearest-neighbor interactions becomes insignificant to the overall electronic coupling through the hydrocarbon spacer. Therefore, the effect of these modifications is to disrupt the electronic coupling through the hydrocarbon network by decreasing these near-neighbor interactions at the modification. In this light one could predict that *any single chemical modification* which permits close packing of the thiol monolayer *should decrease the electronic coupling* through the monolayer. The extent of the decrease would depend on the energy and spatial overlap mismatch between the modification and the polymethylene chain.

In order to predict quantitatively the effect of these modifications on the long-range electronic coupling, we have first calculated the neutral triplet diradical splitting energies for  $\bullet\text{CH}_2-(\text{CH}_2)_n-\text{X}-(\text{CH}_2)_n-\text{CH}_2\bullet$ , where X is the centrally located chemical modification. For these unrestricted Hartree-Fock calculations, we have employed a 3-21G basis set which has been shown to be the simplest basis set which produced reasonable electronic coupling estimates.<sup>11</sup> A more flexible 6-31G<sup>++</sup> basis set was found to produce results within 20% of those obtained using the 3-21G basis set. For each of the structures shown in Table 2, the energy differences between the two highest occupied radical orbitals,  $\Delta E_{\text{cat}}$ , and the two lowest unoccupied radical orbitals,  $\Delta E_{\text{an}}$ , are averaged to give a measure of the electronic coupling through the hydrocarbon chains.<sup>25</sup> These calculations were repeated changing the donor/acceptor reporter orbitals from carbon centered radicals to a pair of nonbonded Li atom radicals separated by 4 Å from the terminal hydrogens of the  $\text{CH}_3(\text{CH}_2)_n-\text{X}-(\text{CH}_2)_n\text{CH}_3$  molecule. The 4 Å separation was chosen to minimize bonding interactions between the Li atoms and the hydrocarbon orbitals. At smaller separation distances, the energy levels for the hydrocarbon orbitals change significantly upon addition of the Li atoms. The purpose of this change in the calculation was to mimic more closely the donor/acceptor structure of the monolayer experiments.

These *ab initio* electronic coupling estimates are compared with the experimental results in Table 2. In the Fermi's golden

(25) This is the Koopman's theorem approach. It should be noted that only the relative magnitude of this coupling energy versus the unmodified hydrocarbon chain is required in this analysis.

rule limit, the square of the electronic coupling energy is proportional to the probability of long-range electron transfer through the hydrocarbon spacer.<sup>26</sup> The squared ratio of the electronic coupling energies between the modified and unmodified hydrocarbons is compared to the average ratio of the heterogeneous electron transfer rate constants measured in Figures 2 and 3.<sup>27</sup> For the ether and olefin modified monolayers, one can observe that the two *ab initio* estimates correctly predict a decrease in the electronic coupling. The size of these predicted decreases are also in reasonable agreement with the experimentally observed values. The agreement between theory and experiment for the alkyne modification depends on the details of the *ab initio* calculation. Using covalently bonded methylene radical reporter groups, the electronic coupling through the alkyne modified hydrocarbon is predicted to be greatly enhanced relative to the unmodified hydrocarbon. In contrast, when the nonbonded Li atoms are used for the donor and acceptor, the calculation is in better agreement with the experimental findings.

The difference in the two *ab initio* estimates for the alkyne electronic coupling is most likely due to the difference in the symmetry of the reporter donor and acceptor groups. The  $\pi$  radical orbitals are more directional than the 2s orbitals of the Li atoms. In the calculation using the  $\pi$  radical orbitals, the orientation of the  $\pi$  radical orbitals with respect to each other and the central modification was found to affect dramatically the electronic coupling estimates in agreement with previous studies.<sup>11</sup> There appears to be a long-range coupling between parallel  $\pi$  orbitals which greatly enhances the overall electronic coupling estimate.<sup>28</sup> This is essentially an artifact of the calculation which we have tried to eliminate. We have varied the length of the hydrocarbon chain from 5 to 14 carbons to determine if a greater separation between the  $\pi$  orbitals would eliminate this effect. We see the same anomalously high coupling estimate from the diradical calculation. A second change made was to increase the flexibility of the basis set used to perform the calculation. We find that using either a 4-31G\* or a 6-31G++ basis set<sup>29</sup> does not markedly affect the high relative electronic coupling prediction. These calculations

highlight the importance of selecting appropriate model structures for the estimation of the electronic coupling.

## Conclusions

Some of the most fundamental aspects of long-range electron transfer can be studied with surprising experimental ease using these self assembled  $\omega$ -hydroxyalkanethiol monolayers. Features advantageous for the study of long-range electron coupling in this electrochemical system include the simplicity of introducing single or multiple point modifications to the alkyl chains and the ability to measure both oxidative and reductive electron transfers over a continuous range of voltages.<sup>30</sup> In this work we find that single atom or bond changes within a hydrocarbon spacer lead to significant decreases in the long-range electronic coupling. The modulation in the electronic coupling occurs even though the number of covalent bonds has not been changed. The approximation commonly used in theoretical studies of electronic coupling through proteins that all covalent bonds should display the same electronic coupling,<sup>31</sup> while reasonable in a global treatment of protein electron transfer, breaks down at the local level. The electronic coupling is observed to be a complex function of the structure of the intervening medium at the atom level.

We are continuing these studies to probe the range of modifications which can be introduced within these monolayers without destroying their ability to act as tunneling barriers. Because the ability to place even a few modifications at specific sites within these monolayers opens up a very large number of possible monolayer structures, the development of predictive theories is clearly needed to aid in designing combinations of modifications which impart useful electronic properties to these monolayers. Important future directions include probing quantum interference effects in monolayers composed of two or more compatible thiols and designing molecule-based current rectification and optical transducers based on these thiol tunneling barriers.

**Acknowledgment.** The authors gratefully acknowledge financial support from the National Association of Corrosion Engineers, the Petroleum Research Fund, and the National Science Foundation (CHE-9417357, CHE-9503348).

JA953210Y

(26) Marcus, R. A.; Sutin, N. *Biochim. Biophys. Acta* **1985**, *811*, 265–322.

(27) We are comparing the electronic coupling calculated for a single hydrocarbon chain with the measured coupling through an assembly of  $\omega$ -hydroxyalkanethiol monolayers. Given that the intermolecular electronic coupling is likely to be much weaker than the intramolecular electronic coupling, this simplification is a reasonable starting point.

(28) It is interesting to note that for the olefin calculation, the reporter orbitals were held perpendicular to the olefin  $\pi$  orbitals which eliminates this coupling pathway accounting for the good agreement with the observed relative electronic coupling.

(29) (a) Ditchfield, R.; Hehre, W. J.; Pople, J. A. *J. Chem. Phys.* **1971**, *54*, 724–728. (b) Hehre, W. J.; Ditchfield, R.; Pople, J. A. *J. Chem. Phys.* **1972**, *56*, 2257–2261. (c) Hariharan, P. C.; Pople, J. A. *Mol. Phys.* **1974**, *27*, 209–214. (d) Gordon, M. S. *Chem. Phys. Lett.* **1980**, *76*, 163–168. (e) Hariharan, P. C.; Pople, J. A. *Theor. Chim. Acta* **1973**, *28*, 213–222. (f) Petersson, G. A.; Bennett, A.; Tensfeldt, T. G.; Al-Laham, M. A.; Shirley, W. A.; Mantzards, J. *J. Chem. Phys.* **1988**, *89*, 2193–2218. (g) Petersson, G. A.; Al-Laham, M. A. *J. Chem. Phys.* **1991**, *94*, 6081–6090.

(30) The potential control afforded by this electrochemical system allows one to probe how electric fields within the tunneling barrier affect the long-range coupling. Such control should allow one to probe the relative importance of electron and hole tunneling in the long-range electron transfer. For these modifications, we observe little potential dependence of the electronic coupling suggesting that both electron and hole mechanisms are equally operative.

(31) (a) Beratan, D. N.; Onuchic, J. N.; Hopfield, J. J. *J. Chem. Phys.* **1987**, *86*, 4488–4498. (b) Beratan, D. N.; Betts, J. N.; Onuchic, J. N. *Science* **1991**, *253*, 1285–1288. (c) Wuttke, D. S.; Bjerrum, M. J.; Winkler, J. R.; Gray, H. B. *Science* **1992**, *256*, 1007–1009. (d) Regan, J. J.; Risser, S. M.; Beratan, D. N.; Onuchic, J. N. *J. Phys. Chem.* **1993**, *97*, 13083–13088. (e) Ullmann, G. M.; Kostic, N. M. *J. Am. Chem. Soc.* **1995**, *117*, 4766–4774.